




Fullerenol as a novel therapeutic agent for sepsis-induced cardiomyocytes damage

Tingjun Zhang^{1,2,6} · Ling Chen^{1,3} · Xuefeng Ding^{1,4} · Rendong He⁵ · Hao Wang³ · Junsong Guo³ · Shaowei Niu² · Guixia Wang⁶ · Fengjun Liu² · Houxiang Hu^{1,3} 

Received: 2 November 2023 / Accepted: 17 January 2024 / Published online: 23 February 2024
© The Author(s) 2024

Abstract

Sepsis-induced myocardial damage (SIMD) is a serious complication of sepsis that affects cardiac function and prognosis. However, effective methods for the prevention and treatment of SIMD are presently lacking. This study reports the crucial function of fullerenols in protecting cardiomyocytes from septic injury. First, we applied the as-prepared fullerenols as an effective free radical scavenger and broad-spectrum anti-oxidant to protect against LPS-induced cardiomyocyte injury. Next, we verified their ability to downregulate IL-6, TNF- α , and ROS-dependent pyroptosis in AC16 induced by LPS. Finally, we observed that the protective mechanism of fullereneol against SIMD involves the regulation of the NF κ B/iNOS/COX-2 pathway. This study presents a timely and essential investigation of the prevention and treatment of SIMD, providing new insights into the applications of fullerenols for therapeutic strategies.

Keywords Sepsis-induced heart disease · Nanoparticles · Fullereneol · Nanomedicine · Myocardial injury

Tingjun Zhang, Ling Chen, and Xuefeng Ding have contributed equally to this work.

✉ Houxiang Hu
hhxiang@nsmc.edu.cn

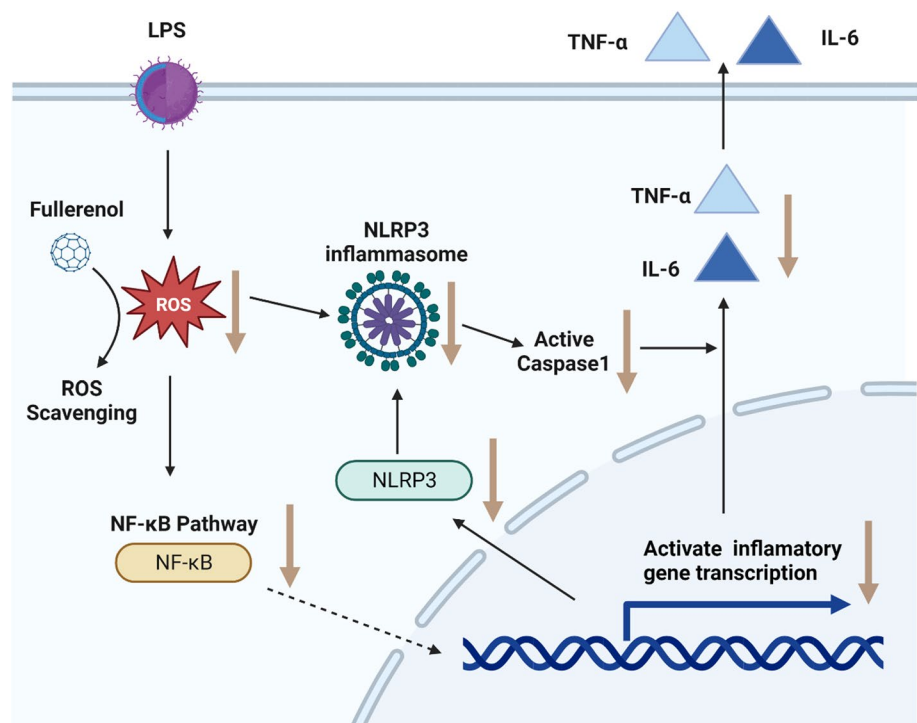
- ¹ First Clinical Medical College, Jinan University, Guangzhou 510632, People's Republic of China
- ² Department of Infectious Diseases, Affiliated Hospital of North Sichuan Medical College, Nanchong 637000, People's Republic of China
- ³ Department of Cardiology, Affiliated Hospital of North Sichuan Medical College, Nanchong 637000, People's Republic of China
- ⁴ Department of Critical Care Medicine, Affiliated Hospital of North Sichuan Medical College, Nanchong 637000, People's Republic of China
- ⁵ Department of Clinical Laboratory, Affiliated Hospital of North Sichuan Medical College, Nanchong 637000, People's Republic of China
- ⁶ Department of Infectious Diseases, Chengdu Third People's Hospital, Chengdu 610036, People's Republic of China

1 Introduction

Sepsis is a leading cause of morbidity and mortality worldwide, affecting around 30 million individuals and resulting in 6 million deaths annually [1]. Sepsis-induced myocardial damage (SIMD) independently increases the risk of fatality in septic patients, manifesting in approximately 50% of cases [2]. However, there exists a scarcity of pharmacological interventions that have been proven effective in treating SIMD. Consequently, the prevention and treatment of SIMD are great challenges and a pressing demand exists for novel therapeutic approaches.

To solve the above problems, scientists have conducted exploratory basic research on this subject and have made some progress. In sepsis, the excessive production of reactive oxygen species (ROS) and the depletion of antioxidants contribute to the development of myocardial injury [3]. Based on this theory, Resveratrol was found to be an antioxidant, anti-inflammatory, and proapoptotic compound, and could potentially be a septic myocardial injury protector [4]. Melatonin, secreted by the pineal gland, has the function of regulating apoptosis, autophagy, and improving mitochondria, implying the ability to protect against myocardial injury [5]. ZHAO et al. found that Kudzu celery decoction has a protective effect on SIMD because of anti-inflammatory,

Scheme 1 Schematic diagram of NLRP3 inflammasome activation induced by LPS. LPS exposure induced ROS generation that could up-regulate NF- κ B pathway to modulate NLRP3 inflammasome activation in AC16 cells. Fullereneol scavenges ROS to inhibit the NF- κ B signaling pathway and thereby modulate NLRP3 inflammasome activity. LPS lipopolysaccharide, ROS reactive oxygen species



anti-oxidative, and other biological activities [6]. Nevertheless, disadvantages hinder the clinical utility of the aforementioned drugs. Resveratrol's low oral bioavailability and rapid metabolism are the major drawbacks of resveratrol [7]. Melatonin has a short half-life of about 20–50 min [8]. Kudzu celery decoction makes it hard to identify its biological targets and interaction mechanisms due to its extreme chemical complexity [9]. Therefore, the challenges of prevention and treatment of SIMD still remain and the development of novel septic myocardial injury protection agents is urgently needed.

Recently, fullerenols has attracted the attention of scientists for its powerful ability to scavenge oxygen and nitrogen free radicals. As a water-soluble derivative of fullerene, fullereneol holds immense potential as a novel nanoprotector for SIMD. This is attributed to three key factors. First, Fullereneol exhibits remarkable free radical scavenging capabilities with its robust delocalized π -conjugated structure and an abundance of hydroxyl groups. This property, often called “free radical sponges”, highlights its potential for highly efficient and broad-spectrum radical elimination [10]. Second, fullereneol showed a propensity to accumulate in the heart, rendering it particularly well suited for safeguarding cardiac tissue from sepsis [11]. Third, fullereneol exhibited good oral utilization [12], long retention in vivo [13], exceptional chemical stability [14], and remarkable biocompatibility [15].

To validate whether fullereneol could be a potential septic protector for SIMD and investigate the protection

mechanism, we employed fullereneol as a shield against SIMD for the first time. In this study, we demonstrate that fullereneol exhibits potent scavenging activities against high ROS, effectively restraining the levels of inflammatory cytokines, including Interleukin-6 (IL-6) and tumor necrosis factor- α (TNF- α), and ROS-dependent pyroptosis in Adult Human-derived Cardiomyocytes (AC16) induced by LPS. In addition, this study elucidated that the protective mechanism of fullereneol against SIMD involves the regulation of the NF- κ B/iNOS/COX-2 pathway to modulate NOD-like receptor thermal protein domain-associated protein 3 (NLRP3)-mediated pyroptosis (Scheme 1). Therefore, our findings provide a novel strategy for preventing and treating SIMD and also highlight the promising prospects of fullereneol for translational and practical applications.

2 Materials and methods

2.1 Materials

All reagents were of analytical grade and used without additional purification. 1,1-Diphenyl-2-picrylhydrazyl radical (DPPH) was obtained from Alfa Aesar, while 2,2'-azino-bis 3-ethylbenzthiazoline-6-sulfonate (ATBS) was supplied by Sigma-Aldrich. The 3,3',5,5'-tetramethylbenzidine (TMB) was provided by Tokyo Chemical Industry Co. Ltd. AC16 human-derived cardiomyocytes were offered from Shangcheng Beina Chuanglian Biotechnology Co.

β -Nicotinamide adenine dinucleotide (NADH) and nitroblue tetrazolium chloride (NBT), Cell Counting Kit-8 (CCK-8), Hoechst 33,342, ROS Assay Kit, Alexa Fluor 488-labeled goat anti-mouse IgG (H+L), and GPR49/LGR5 Rabbit Polyclonal Antibody were furnished by Byotime Institute of Biotechnology. Additionally, Beijing Enokai Technology Co. Ltd. provided Cy5. Fullerenol was kindly provided by CAS Key Laboratory for Biomedical Effects of Nanomaterials and Nanosafety, Institute of High Energy Physics, Chinese Academy of Sciences.

2.2 Characterization

The molecular structures of as-prepared fullerenols were characterized by Fourier transform infrared spectrometer (Thermo iN10-iZ10) and X-ray photoelectron spectrometer (XPS, Thermo ESCALAB 250xi). The integrity of the carbon cage was characterized by MALDI-TOF-MS (Bruker UltrafleXtreme). The carbon-carbon double bonds on the carbon cage were studied by a high-resolution Raman spectrometer (HORIBA LabRAM HR Evolution). The hydrodynamic size and zeta potential were measured with a dynamic light scattering (DLS) particle-size analyzer (Brookhaven Omni). Then, the graphs were prepared by Graphpad version 8.0.

2.3 Cell culture

AC16 cells were cultured in Dulbecco's modified eagle medium (DMEM) (GIBCO, USA), enriched with 10% fetal bovine serum (FBS) and 1% penicillin/streptomycin, under a humidified atmosphere consisting of 5% CO₂ and 95% air at 37 °C. Additionally, 0.05% trypsin was utilized for cell digestion, and the medium was refreshed daily. These AC16 cells were exposed to various stimuli in either 6-well plates or 96-well plates.

2.4 Treatment of cells

LPS and fullerenol were dissolved in sterile deionized water at concentrations of 10 μ g/mL and 25 μ g/mL, respectively. The control group was administered sterile saline solution, while the LPS group was exposed to 10 μ g/mL LPS for 24 h. Cells in the fullerenol + LPS group underwent a pre-treatment of 25 μ g/mL fullerenol for 2 h, followed by exposure to 10 μ g/mL LPS for 24 h. The fullerenol group was exclusively exposed to 25 μ g/mL fullerenol for 2 h. Following incubation, cells were harvested and subjected to analysis for lactate dehydrogenase (LDH) levels, ROS levels, cell viability, and protein expression. The culture medium was also assessed for levels of superoxide dismutase (SOD), malondialdehyde (MDA), IL-6, and TNF- α .

2.5 Cell viability

The cell viability in 96-well plates was assessed using the CCK-8 assay kit (Bestbio, Shanghai, China), following the manufacturer's instructions. After a 24-h cell treatment, each well was supplemented with 10 μ L of sterile CCK-8 solution and subjected to a 2-h incubation in darkness at 37 °C. Subsequently, the absorbance at 450 nm was quantified utilizing a microplate reader.

2.6 LDH activity assay

Cell injury was estimated by detecting LDH activity using an LDH assay kit (BeastBio, Shanghai, China), in accordance with the manufacturer's instructions.

2.7 Enzyme-linked immunosorbent assay (ELISA)

The concentrations of inflammatory cytokines, including TNF- α and IL-6, as well as oxidative stress biomarkers like SOD and MDA, were determined using commercially available ELISA kits (Jianglai, Shanghai, China).

2.8 Measurement of ROS generation

Intracellular ROS levels were quantified using the fluorescent probe dichloro-dihydro-fluorescein diacetate (DCFH-DA; Sigma, USA). Following stimulation, cells were incubated with DCFH-DA (50 μ M) at 37 °C for 30 min. Subsequently, the cells were washed twice with Phosphate-Buffered Saline (PBS). The data were analyzed utilizing Image J software.

2.9 Western blot

Following stimulation, cells were lysed using radioimmunoprecipitation assay (RIPA) buffer (Beyotime, China) containing a protease inhibitor cocktail (Beyotime, China) that included phenylmethylsulfonyl fluoride (PMSF, Beyotime, China). Subsequently, all homogenates were centrifuged at 12,000 rpm for 15 min at 4 °C. Equal amounts of denatured protein were loaded onto 10% Sodium Dodecyl Sulfate-PolyAcrylamide Gel Electrophoresis (SDS-PAGE) gels. Subsequently, they were transferred onto polyvinylidene difluoride (PVDF) membranes. Membranes were blocked with 5% nonfat milk at room temperature for 1 h. The membranes were then incubated overnight with primary antibodies targeting inducible nitric oxide synthase (iNOS, 1:1000, NOVUS, USA), cyclooxygenase-2 (COX-2, 1:500, Abcam, USA), nuclear factor kappa B (NF- κ B, 1:1000, Abcam, USA), phosphorylated NF- κ B (p-NF- κ B, 1:1000, Abcam, USA), NLRP3 (1:1000, NOVUS, USA), caspase-1 (1:1000, NOVUS, USA), gasdermin D (GSDMD, 1:1000, Abcam,

USA), and glyceraldehyde phosphate dehydrogenase (GAPDH, 1:10,000, Abcam, USA). Subsequently, membranes were incubated with a fluorescent secondary antibody (1:2500, CST, USA) for 2 h at 4 °C. The membranes were washed three times with Tris–HCl Tween buffered salt solution (TBST), each wash lasting 5 min. Protein expression quantification was normalized to GAPDH.

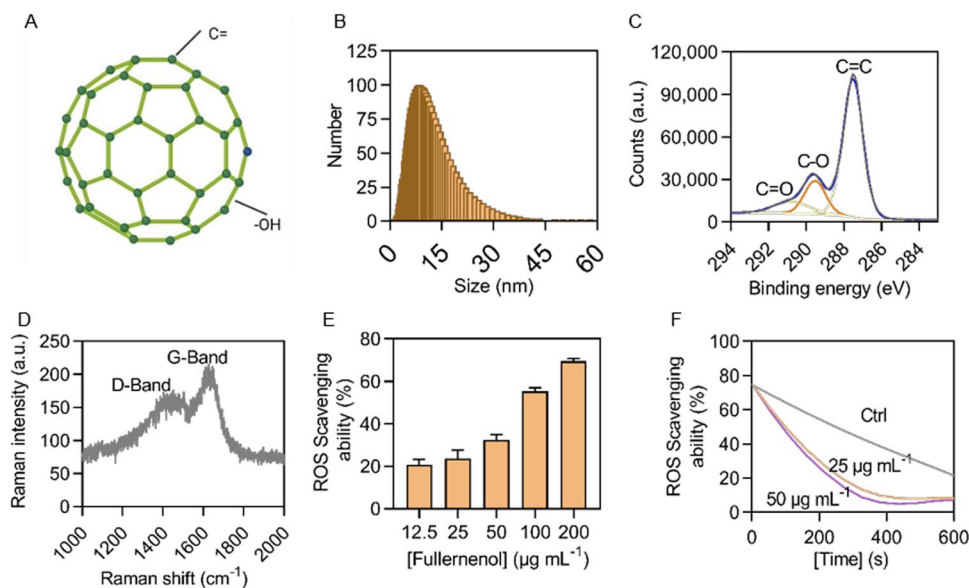
2.10 Propidium iodide (PI) staining

Following stimulation, the cells were collected and thoroughly washed thrice with $1 \times$ PBS. Subsequently, the cells were rinsed with $1 \times$ assay buffer. A solution of 5 μ M PI in $1 \times$ assay buffer was prepared and employed to stain each well, incubating at a temperature of 37 °C for 15 min. In the final step, cells were stained with 4,6-diamino-2-phenyl indole (DAPI, Sigma, USA) for a concise duration of 5 min. Immediate post-staining images of the cells were captured using a fluorescence microscope. The software Image J was deployed to evaluate both the average fluorescence intensity and the percentage of positive cells.

2.11 Statistical analysis

The results are presented as the mean \pm Standard Deviation (SD), with sample size (n) displayed in each figure legend. No data pre-processing was performed. Statistical analyses were conducted using GraphPad Prism version 9.0 (GraphPad Software, USA). Statistical significance between the two groups was analyzed using unpaired, two-tailed Student's *t* test. Multiple-group comparisons were performed using one-way analysis of variance (ANOVA). *P* values < 0.05 were considered statistically significant, and differences were denoted by an asterisk (* or #).

Fig. 1 Characterization and function of fullerene nanoparticles. **A** Molecular structures of $C_{60}(OH)_{22}$ nanoparticles. **B** The hydrodynamic diameter potential of as-prepared fullerene. **C** XPS spectra of as-prepared fullerene. **D** Raman spectra of as-prepared fullerene. **E** ROS scavenging ability of as-prepared fullerene. **F** ROS scavenging ability of as-prepared fullerene in different time points



3 Results and discussion

3.1 Characterization and free radical scavenging activity of fullerene

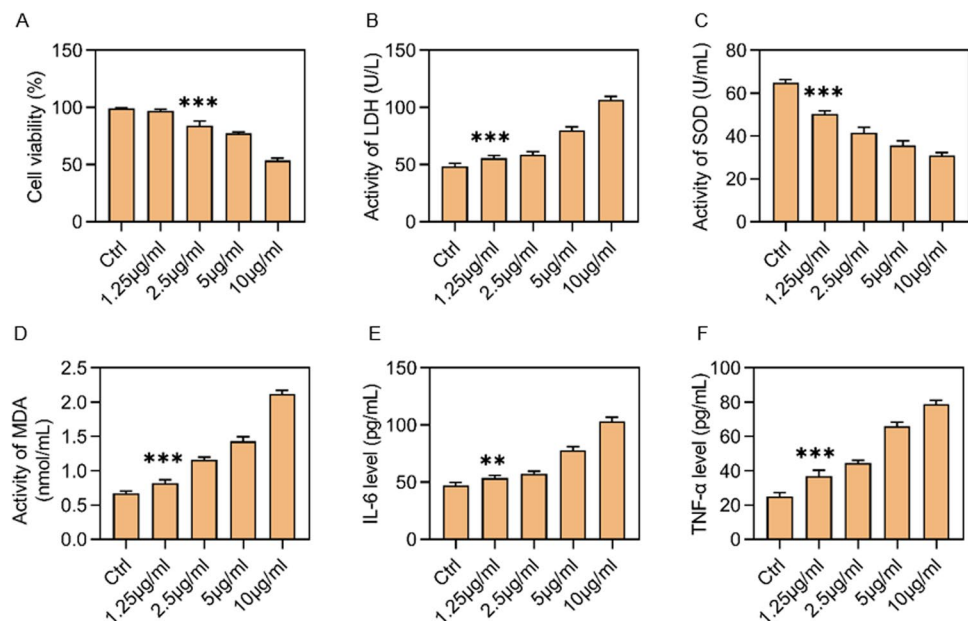
Fullerene is a fullerene derivative with a spherical carbon cage structure (Fig. 1A) [16]. The fullerenols used in this study were synthesized using an environmentally friendly and scalable method. This process involved wet ball milling with hydrogen peroxide (H_2O_2) aqueous solution serving as the hydroxylation agent, and a small amount of sodium hydroxide (NaOH) acting as a catalyst [17]. The as-prepared fullerene exhibited a particle size of 5–10 nm, aligning with the data on hydrodynamic diameter (Fig. 1B). The zeta potential of the fullerene was determined to be -45 mV in absolute terms (Fig. S1A). XPS was employed to ascertain the elemental composition and bonding energy of the as-prepared fullerene. As illustrated in Fig. 1C, the peaks centered at 285 eV, 287 eV, and 289 eV correspond to C=C, C–O, and C=O bonds, respectively. The structural identity of the fullerenols was further elucidated through rigorous analysis using Fourier Transform Infrared Spectroscopy (FTIR) and Raman Spectroscopy. The FTIR spectra of the as-prepared fullerene revealed four distinct absorption peaks at 3405, 1615, 1365, and 1082 cm^{-1} , which correspond to the skeletal vibrations of O–H, C=C, C–O–H, and C–O bands, respectively (Fig. S1B). Subsequently, the Raman spectrum displayed two prominent peaks at 1357.46 cm^{-1} and 1598.34 cm^{-1} , consistent with the D and G bands of C–C on the carbon cage of fullerene (Fig. 1D). The results from both FTIR and Raman spectroscopy confirmed the successful integration of hydroxyl groups into

the carbon cages, leading to the formation of hydroxylated fullerenes [18]. These results provide compelling evidence for the abundant presence of oxidizing groups on the surface of the fullerene's carbon cage [19]. As depicted in Fig S1A, the XPS results underscore the high purity of the as-prepared fullerene, with only carbon and oxygen elements detected, devoid of harmful impurities. These findings collectively affirm the successful synthesis of fullerenols. Subsequently, we evaluated the fullerene's capacity to scavenge reactive oxygen species/reactive nitrogen species (ROS/RNS) and its potential as a septic protective agent for the heart. Fullerenols demonstrated commendable ROS scavenging performance. Remarkably, the scavenging rates of these free radicals reached 23.71% and 89.37% at fullerene concentrations of 25 $\mu\text{g/mL}$ and 200 $\mu\text{g/mL}$, respectively (Fig. 1E). The peak scavenging rate was achieved within approximately 400 s (Fig. 1F). Fullerene also exhibited a potent inhibitory effect on the model nitrogen radicals DPPH and ABTS in a concentration-dependent manner (Fig. S2A-B). Moreover, they effectively suppressed the superoxide anions ($\text{O}_2^{\bullet-}$) generated by the nicotinamide adenine dinucleotide (NADH)/phenazine methosulfate (PMS) reaction. They prevented the conversion of nitro-blue tetrazolium chloride (NBT) into blue formazan (Fig S2C). Additionally, fullerenols were able to inhibit the generation of hydroxyl radicals ($\bullet\text{OH}$) from Fenton's reaction. They obstructed the synthesis of oxidized 3,3',5,5'-tetramethylbenzidine (oxTMB) (Fig S2D), thereby reducing the absorption at 652 nm. As a consequence, the above results suggest that the extensive free radical scavenging activity makes fullerene a potential to act as a nanoprotector against SIMD.

3.2 Protective effect of fullerene on LPS-induced cardiomyocytes damage

To ascertain the impact of LPS on cardiomyocyte activity and LDH release, AC16 cells were exposed to varying concentrations of LPS, followed by an assessment of cell viability and LDH release. The findings revealed an inverse correlation between AC16 cell viability and LPS concentration. As the LPS concentration elevated, the viability of AC16 cells diminished, with a notable decrease observed in cells exposed to 2.5 $\mu\text{g/mL}$ LPS (Fig. 2A). Moreover, LDH release exhibited a direct correlation with LPS concentration (Fig. 2B). The higher the LPS concentration, the more substantial the LDH release, with the maximum release observed in cells treated with 10 $\mu\text{g/mL}$ LPS. It is noteworthy that even minimal LPS concentrations significantly influenced myocardial cells. Then, a series of experiments were conducted to extensively investigate the effects of LPS on the oxidative stress biomarkers and inflammatory cytokines present in the supernatant of AC16 cardiomyocytes. Our results determined a negative correlation between LPS concentration and SOD activity (Fig. 2C), indicating a considerable influence of LPS on intracellular anti-oxidant enzyme activities. Additionally, we observed a positive correlation between LPS concentration and the lipid peroxidation product malondialdehyde MDA (Fig. 2D), suggesting an essential effect of LPS on AC16 cell oxidative stress status. Furthermore, our observations showed a positive correlation between IL-6 and TNF- α levels and LPS concentration (Fig. 2E, F), affirming the critical role of LPS as an inflammatory mediator in triggering the cellular inflammatory response. Then, the effect of fullerene on LPS-induced cardiomyocytes damage was investigated. Initially, the safety

Fig. 2 Dose-dependent effects of LPS on AC16 cells. **A** The cell viability of AC16 impacted by LPS. **B** The level of LDH affected by LPS. **C** The activity of SOD impacted by LPS. **D** The MDA content affected by LPS. **E** The levels of inflammatory cytokines IL-6 affected by LPS. **F** The levels of inflammatory cytokines TNF- α affected by LPS. Data are shown as mean \pm standard deviation (SD) ($n=6$). * $P < 0.05$ and *** $P < 0.01$ compared to control group



of fullereneol was evaluate via assessing its impact on cellular activity utilizing CCK-8 assay. The results showed no significant changes in cell viability and LDH release under diverse concentrations of fullereneol (12.5–100 $\mu\text{mol/L}$) treatment (Fig. 3A, B), indicating the low toxicity of fullereneol toward AC16 cells. Then, we investigated the protective potential of fullereneol in LPS-induced cardiomyocytes injury. Our findings demonstrated that pre-treatment with fullereneol for 2 h significantly protected the cells from LPS-induced injury by promoting the restoration of cell viability and minimizing the release of LDH in a concentration-dependent fashion (Fig. 3C, D). Notably, the protective inhibition was observed at a concentration of 25 $\mu\text{mol/L}$, reiterating its efficacy. In the present study, we found that LPS-induced reduction in cardiomyocyte activity and release of LDH was attenuated by fullereneol, suggesting that fullereneol has a protective effect on damaged cardiomyocytes. In fact, protective effect of fullereneol for cardiovascular disease has been performed before. For example, fullereneol has the ability to attenuate oxidative stress by quenching ROS to alleviate radiation-induced cyocardial injury [20]. Ding et al. found that fullereneol can mitigate myocardial ischemia–reperfusion injury by reducing the expression of inflammatory factors in rats

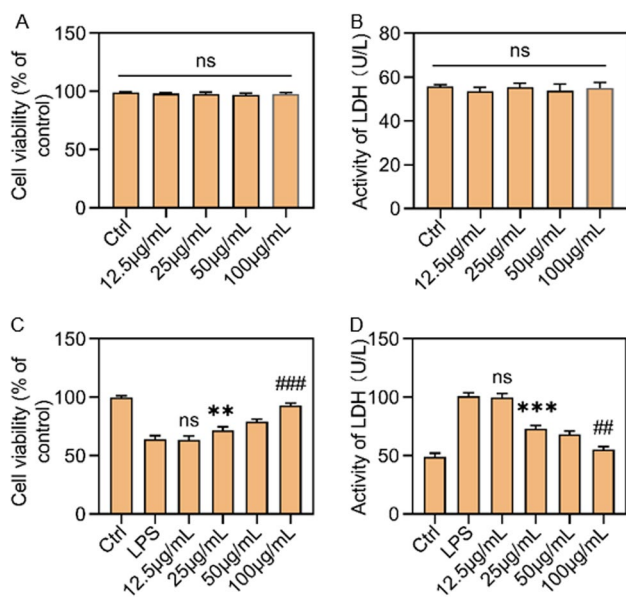


Fig. 3 The effect of fullereneols (Fu) on cell viability and LDH release in LPS-treated AC16 cells. **A** The toxicity of Fu on cells was measured using the CCK-8 assay. **B** The activity of LDH affected by Fu was measured using the LDH assay. **C** The effects of fullereneols on LPS-induced AC16 cell injury were detected using the CCK-8 assay. Data are shown as mean \pm SD ($n=6$). ** $P < 0.01$ compared to LPS group; ### $P < 0.01$ compared to control group; ns, $P > 0.05$ compared to control group. **D** The effects of fullereneol on LPS-induced AC16 cell injury were detected using the LDH assay. Data are shown as mean \pm SD ($n=6$). ** $P < 0.01$ compared to control group; ### $P < 0.01$ compared to LPS group; ns, $P > 0.05$ compared to control group

and improving the anti-oxidative capacity of cardiomyocytes [13]. The present study confirms the protective effect of fullereneol in septic myocardial injury and provides a new strategy for the development of protective agents against septic myocardial injury.

3.3 The mechanism of protective effect of fullereneol on LPS-induced cardiomyocytes damage

Inspired by the protective effect of fullereneol on cardiomyocytes, we investigated the precise involvement of ROS in LPS-induced myocardial injury. The administration of LPS led to elevated levels of intracellular ROS and MDA while suppressing SOD activity. As shown in Fig. 4A–C and D, pre-treatment with fullereneol effectively attenuated intracellular ROS and MDA production while augmenting SOD activity. These findings strongly imply the vital contribution of ROS in developing LPS-induced myocardial injury, indicating the efficacy of fullereneol in diminishing ROS production and boosting anti-oxidant capacity, consequently mitigating myocardial injury. In addition, the number of dead cardiomyocytes was increased significantly with LPS-stimulated ROS production and inflammatory cytokine stimulation. Nevertheless, by reducing ROS production, fullereneol exhibited a remarkable capacity to attenuate cell death (Fig. 5). Our findings demonstrate that fullereneol could ameliorate LPS-induced cellular injury by scavenging ROS, reducing MDA production, and increasing the activity of the anti-oxidant enzyme SOD. Fullereneol scavenges ROS, a key molecule in the process of LPS, leading to cardiomyocyte injury, thereby attenuating myocardial damage caused by sepsis. Oxidative stress, a critical mechanism implicated in cardiovascular diseases, including myocardial injury [5], arises predominantly from excessive ROS generation during LPS-induced myocardial cell injury [21]. ROS adversely impacts essential cellular constituents and macromolecules

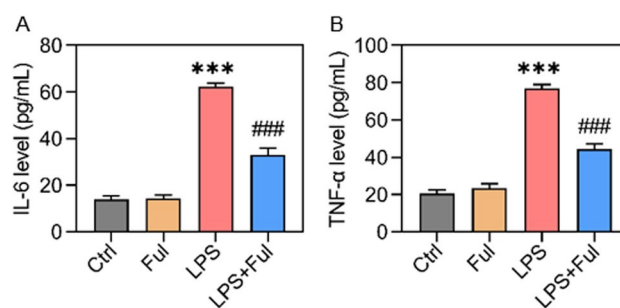


Fig. 4 Protective effect of fullereneols to the cell injury of AC16s exposed to LPS. **A** The levels of inflammatory cytokine IL-6, detected by ELISA. **B** The levels of inflammatory cytokine TNF- α , detected by ELISA. Data are shown as mean \pm SD ($n=6$). *** $P < 0.001$ compared to control group; ### $P < 0.001$ compared to LPS group; ns, $P > 0.05$ compared to control group

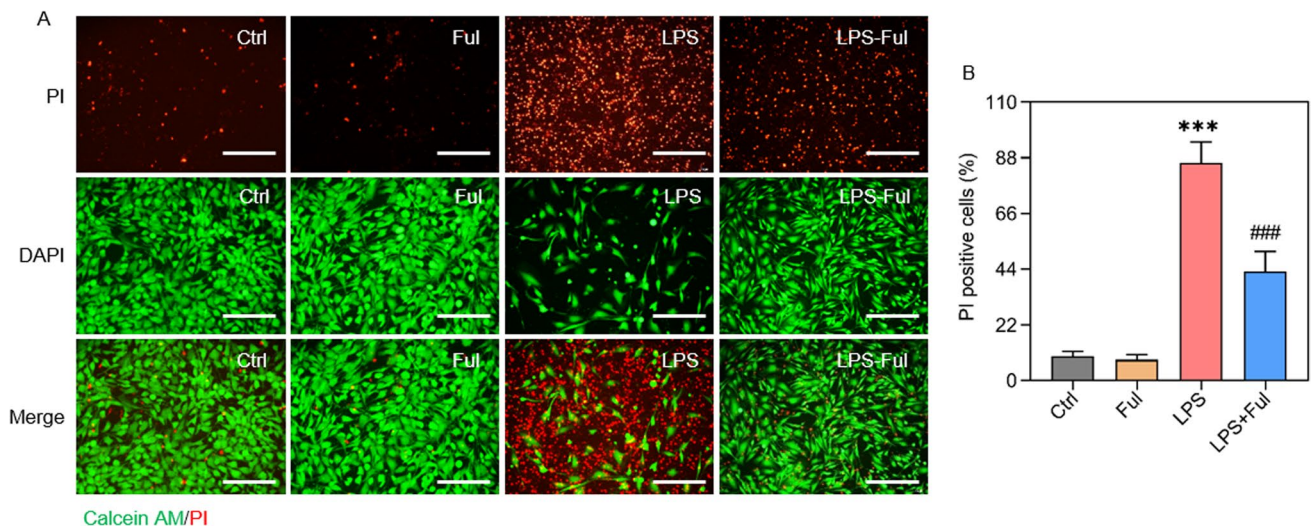


Fig. 5 The effect of fullereneol on pyroptotic in AC16 cells after LPS treatment. **A** Fluorescence images of pyroptotic cells in different groups. Pyroptotic cells were detected using PI staining (scale bar:

400 μ m. 100 \times magnification). **B** The percentage of PI positive cells in different groups. Data are shown as mean \pm SD; *** P < 0.001 compared to control group; ### P < 0.001 compared to LPS group; n = 3

such as proteins and DNA [22]. Moreover, it precipitates a decline in the activity of crucial anti-oxidant enzymes, notably SOD [23], thereby intensifying the burden of oxidative stress. This cellular damage further triggers mitochondrial dysfunction, thereby exacerbating tissue injury [24]. Our results suggest that fullereneol can improve cellular activity by inhibiting ROS-dependent cell death, which provides a novel avenue for further exploration of the role of fullereneol in treating cardiovascular diseases. Upon meticulous examination of the preceding experiments, we arrived at the compelling conclusion that fullereneol can mitigate LPS-induced injury of AC16 cells by curtailing the production of intracellular ROS. To further explore this mechanism, we assessed the protective effects of fullereneol against ROS-dependent pyroptosis in LPS-treated AC16 cells by measuring essential proteins of pyroptosis, namely NLRP3, caspase-1, and GSDMD, in subsequent experiments. Remarkably, our findings showed a substantial escalation in the expression of NLRP3, caspase-1, and GSDMD upon LPS treatment, compared to the control group (Fig. 6A–D). This resoundingly affirmed the existence of a consequential ROS-dependent pyroptosis phenomenon in AC16 cells under LPS treatment conditions. However, this deleterious effect was efficiently counteracted through the pre-administration of fullereneol. Specifically, NLRP3, caspase-1, and GSDMD expression significantly decreased after pre-treatment with fullereneol, suggesting that fullereneol can effectively protect cells from ROS-dependent pyroptosis. It was demonstrated that pre-treatment with fullereneol effectively mitigated ROS production, resulting in a notable reduction in the expression of NLRP3, caspase-1, and GSDMD proteins. Upon stimulation by pathogen-associated molecular patterns (PAMPs), the

NLRP3 inflammasome can be activated via an ROS-dependent signaling pathway [25]. ROS, a crucial signaling molecule, is known to facilitate inflammasome activation and plays a key role in activating the NLRP3/caspase-1 complex [26], consequently triggering cellular pyroptosis [27]. Under normal physiological conditions, anti-oxidant enzymes scavenge ROS during cellular metabolism to maintain a balance between ROS production and elimination [28]. Nevertheless, the sustained production of ROS disrupts intracellular redox homeostasis, ultimately leading to oxidative stress injury and cellular damage, including apoptosis [29], and pyroptosis [27]. Therefore, fullereneol may exert a protective effect through its anti-oxidant properties to reduce ROS production and thus alleviate NLRP3-mediated pyroptosis in AC16 cardiomyocytes.

Motivated by the efficient protective effects of fullereneol for AC16 cells, the effect of fullereneol on inflammatory cytokines in AC16 cells was further evaluated, since inflammatory responses and cytokine release facilitated LPS-mediated cellular injury. Following LPS treatment, the cell supernatant's expression of inflammatory cytokines (IL-6, TNF- α) noticeably increased. Conversely, pre-treatment with fullereneol (25 μ mol/L) inhibited the levels of IL-6 and TNF- α , as demonstrated in Fig. 7A and B. It was found that fullereneol reduced the production of ROS during oxidative stress while enhancing the viability of AC16 cardiomyocytes by decreasing the release of inflammatory cytokines (such as TNF- α and IL-6). Oxidative stress and inflammatory response are intricately linked to cardiac insufficiency and sepsis [30]. Notably, IL-6 and TNF- α , classified inflammatory cytokines, emerge as the main medium for cardiac dysfunction in sepsis [31]. Noteworthy clinical and

Fig. 6 The effect of fullerlenols on the expression of NLRP3, caspase-1, and GSDMD in LPS-treated AC16 cells. **A** Representative and averaged Western blot analysis NLRP3, caspase-1, and GSDMD in AC16. A “+” symbol indicates presence and a “-” symbol indicates the absence of the relevant treatment. **B** The relative protein expression levels of NLRP3/GAPDH. **C** The relative protein expression levels of caspase-1/GAPDH. **D** The relative protein expression levels of GSDMD/GAPDH. Data are shown as mean \pm SD ($n=3$). $^{***}P < 0.01$ compared to control group; $^{\#}P < 0.05$ compared to LPS group; $^{\#\#}P < 0.01$ compared to LPS group

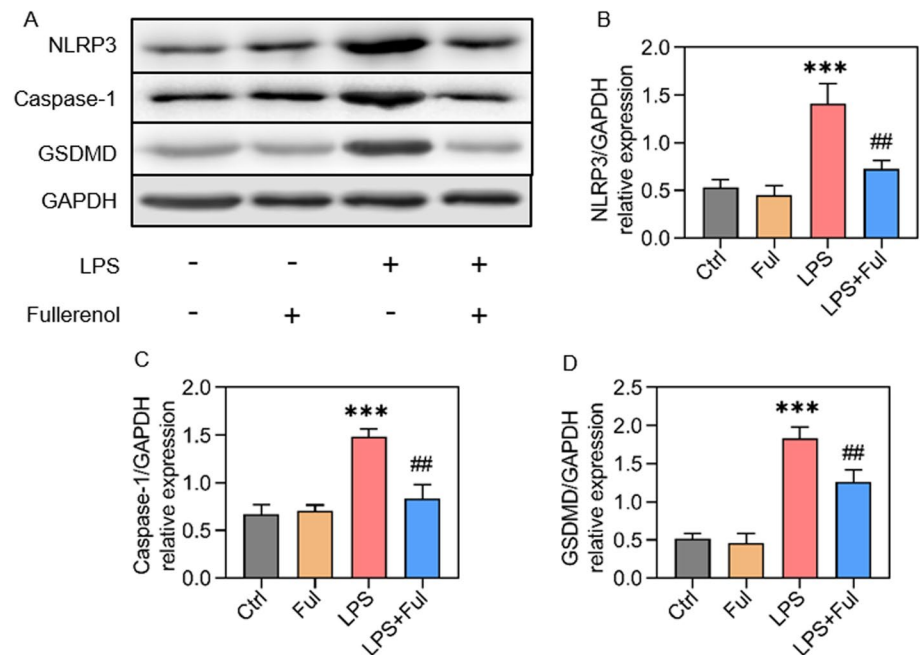
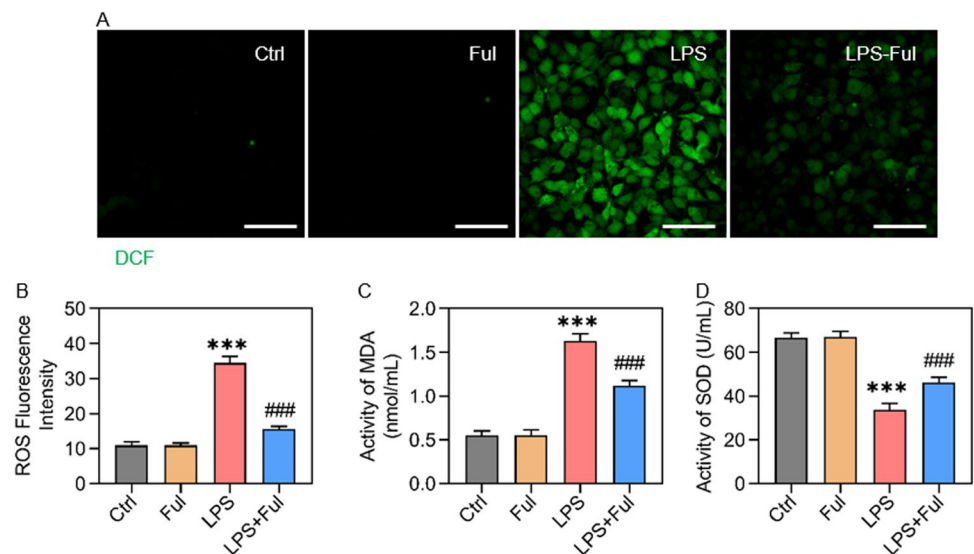


Fig. 7 Protective effect of fullerlenols to the oxidative stress of AC16s exposed to LPS. **A** Fluorescence images of ROS in different groups. **B** The effect of fullerlenols on the levels of intracellular ROS. **C** The levels of MDA in AC16 cells exposed or not exposed to LPS. **D** The activity of SOD in AC16 cells exposed or not exposed to LPS. Data are shown as mean \pm SD ($n=6$). $^{***}P < 0.001$ compared to control group; $^{\#\#\#}P < 0.001$ compared to LPS group; ns, $P > 0.05$ compared to control group; scale bar, 800 μ m



experimental studies have unequivocally demonstrated that inflammatory cytokines exacerbate sepsis-induced cardiac dysfunction [32], whereas inhibiting their activity can ameliorate such dysfunction in sepsis animal models and human patients [33]. Moreover, our investigation has revealed that fullerlenol possesses the capability to attenuate the LPS-induced inflammatory response by effectively reducing the release of inflammatory cytokines. This finding provides supplementary evidence affirming the potential of fullerlenol as a prospective therapeutic agent for sepsis.

To further explore the intricate mechanisms underlying the cardioprotective effects of fullerlenol against LPS-induced injury, we meticulously scrutinized the protein

expression of inducible nitric oxide synthase (iNOS) and COX-2 in AC16 cells, as well as the activation of NF- κ B. Our findings unveiled a significant upregulation in the levels of iNOS, COX-2, and phosphorylated NF- κ B (p-NF- κ B) after LPS exposure. Notably, the introduction of fullerlenol effectively reversed this response, as evidenced by the observed down-regulation of iNOS, COX-2, and p-NF- κ B (Fig. 8A–E). Our experimental results unveiled the remarkable ability of fullerlenol to effectively impede the upregulation of iNOS, COX2, and p-NF- κ B in LPS-induced myocardial injury. Hence, the protective effect of fullerlenol can be attributed to its potent anti-inflammatory properties. The inflammatory response consequentially promotes

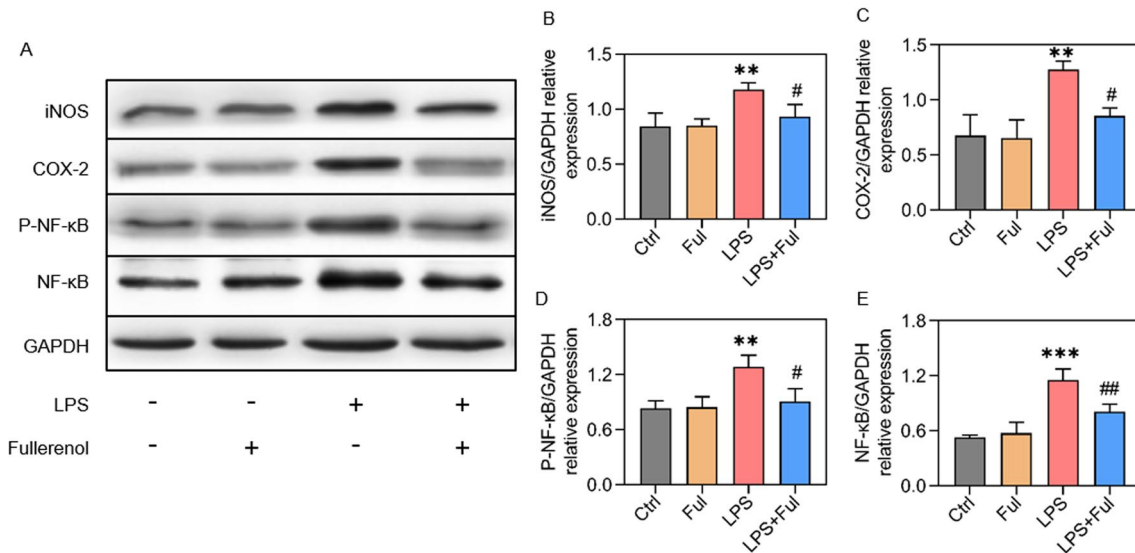


Fig. 8 The effect of fullereneol on the expression of iNOS, COX-2, p-NF-κB, and NF-κB in LPS-treated AC16 cells. **A** Representative and averaged Western blot analysis for iNOS, COX-2, NF-κB, and p-NF-κB in AC16. A “+” symbol indicates presence and a “-” symbol indicates the absence of the relevant treatment. **B** The relative protein expression levels of iNOS/GAPDH. **C** The relative protein

expression levels of COX-2/GAPDH. **D** The relative protein expression levels of p-NF-κB/GAPDH. **E** The relative protein expression levels of NF-κB/GAPDH in AC16 cells. Data are shown as mean \pm SD ($n=3$). ** $P < 0.01$ compared to control group; # $P < 0.05$ compared to LPS group; ## $P < 0.01$ compared to LPS group

the expression of inflammatory cytokines, such as COX-2 and iNOS, as corroborated in prior studies [34]. LPS, being the trigger, instigates the activation of the NF-κB pathway, thereby propelling the inflammatory response [35]. Moreover, phosphorylation NF-κB triggers the liberation and dimerization of NF-κB, which was previously bound to the inhibitory IκB molecule. Consequently, the translocation of NF-κB to the nucleus is facilitated, thereby promoting the transcriptional activity of inflammatory genes and culminating in the release of inflammatory cytokines [36]. This intricate process regulates the inflammatory response and the expression of iNOS and COX-2 [5]. Previous investigations have firmly established that the NF-κB pathway is a primary regulator of iNOS and COX-2 expression, intimately associated with myocardial dysfunction [37]. Furthermore, by diminishing oxidative stress, the expression of COX-2 and iNOS can be subdued through the suppression of the NF-κB pathway, effectively alleviating tissue damage and significantly reducing the extent of the inflammatory response [38]. Hence, the mechanism of fullereneol of anti-inflammatory action in LPS-induced myocardial injury may operate through the elimination of free radical accumulation.

In this study, our results suggest that fullereneol pre-treatment was found to benefit LPS-induced myocardial injury. Initially, fullereneol markedly reduced the ROS generated by LPS, subsequently inhibiting inflammatory responses and diminishing the levels of IL-6, TNF-α, and ROS-dependent pyroptosis. Furthermore, fullereneol suppressed the activation of the NF-κB pathway, leading to a down-regulation in

the expression of inflammatory proteins, including iNOS and COX-2. This also reduced the expression levels of pyroptosis proteins such as NLRP3, caspase-1, and GSDMD in cardiomyocytes. It was confirmed that inflammatory vesicle-mediated cellular pyroptosis is regulated by the NF-κB signaling pathway in the inflammatory response [39]. Regrettably, the protective mechanism of fullereneol in LPS-induced myocardial injury should be further elucidated in an animal model of sepsis, which is a fundamental limitation of this study. Nevertheless, this study identified a novel therapeutic agent, fullereneol. By reducing the production of ROS and MDA and enhancing the activity of the anti-oxidant enzyme SOD, fullereneol can ameliorate LPS-induced cell damage. Additionally, we shed light upon the pivotal role of fullereneol in inhibiting inflammatory responses and ameliorating pyroptosis through scavenging free radicals and modulating NFκB/iNOS/COX-2-dependent pathways for myocardial protection in sepsis (Scheme 1). This groundbreaking study paves the way for a deeper understanding of the myocardial safeguarding mechanisms in sepsis.

4 Conclusion

In summary, for the first time, we investigated the potent cardioprotective effects of fullereneol pretreated against LPS-induced myocardial injury. The observed protective mechanism primarily lies in the notable efficacy of fullereneol in scavenging free radicals. This anti-oxidative property

emerges as a key player in mitigating LPS-induced myocardial injury. Furthermore, our findings suggest that fullereneol may exert its protective influence by intervening in the NF κ B/iNOS/COX-2 pathway. This intervention results in the suppression of inflammatory cytokines, such as IL-6 and TNF- α , and consequently ameliorates ROS-dependent pyroptosis, contributing to the cardioprotective effects observed in our study (Scheme 1). Overall, this study not only implies the potent potential of fullereneol for alleviating SIMD, but also provides a new avenue for the design of sepsis protectors using the advantage of nanomaterials.

Supplementary Information The online version contains supplementary material available at <https://doi.org/10.1007/s00339-024-07315-y>.

Acknowledgements The authors are grateful for the support of the Academician Workstation Fund of Affiliated Hospital of North Sichuan Medical College. The authors are also grateful for the team of Dr. Gu Zhanjun from CAS Key Laboratory for Biomedical Effects of Nanomaterials and Nanosafety, Institute of High Energy Physics, Chinese Academy of Sciences, for their kind help and support.

Author contributions TZ, LC, and XD: conceptualization supporting; formal analysis, investigation, methodology, and writing—original draft leading. RH: data curation, formal analysis, and editing supporting. HW and JG: investigation supporting. SN, GW, and FL: methodology and writing—review supporting. HH: funding acquisition, supervision, and writing—review and editing supporting.

Funding This work was supported by the foundation of the Science and Technology Project of Nanchong (No. 22SXQT0337), and the Science and Technology Project of Affiliated Hospital of North Sichuan Medical College (Nos. 2020ZX003, 2022JB002, and 2022JC028).

Data availability The datasets generated during the current study are available from the corresponding author on reasonable request.

Declarations

Conflict of interest The authors have no competing interests to declare that are relevant to the content of this article.

Open Access This article is licensed under a Creative Commons Attribution 4.0 International License, which permits use, sharing, adaptation, distribution and reproduction in any medium or format, as long as you give appropriate credit to the original author(s) and the source, provide a link to the Creative Commons licence, and indicate if changes were made. The images or other third party material in this article are included in the article's Creative Commons licence, unless indicated otherwise in a credit line to the material. If material is not included in the article's Creative Commons licence and your intended use is not permitted by statutory regulation or exceeds the permitted use, you will need to obtain permission directly from the copyright holder. To view a copy of this licence, visit <http://creativecommons.org/licenses/by/4.0/>.

References

- I.T. Schrijver, C. Théroude, T. Roger, *Front. Immunol.* **10**, 327 (2019). <https://doi.org/10.3389/fimmu.2019.00327>
- W. Mu, Y. Han, G. Gu, C. Yao, *Zhonghua Wei Zhong Bing Ji Jiu Yi Xue* **33**(7), 809 (2021). <https://doi.org/10.3760/cma.j.cn121430-20201225-00774>
- S.R. Senousy, A.F. Ahmed, D.A. Abdelhafeez, M.M.A. Khalifa, M.A.S. Abourehab, M. El-Daly, *Drug Des. Dev. Ther.* **16**, 3023 (2022). <https://doi.org/10.2147/dddt.S370460>
- J. Grujić-Milanović, V. Jačević, Z. Miloradović, D. Jovović, I. Milosavljević, S.D. Milanović, N. Mihailović-Stanojević, *Int. J. Mol. Sci. J. Mol. Sci.* (2021). <https://doi.org/10.3390/ijms22095006>
- Z.D. Su, X.B. Wei, Y.B. Fu, J. Xu, Z.H. Wang, Y. Wang, J.F. Cao, J.L. Huang, D.Q. Yu, *Ann. Transl. Med.* **9**(5), 413 (2021). <https://doi.org/10.21037/atm-20-8196>
- L. Zhao, H. Zhao, M. Sun, M. Chen, X. Wu, C. Deng, W. Yang, Y. Tian, Q. Wang, Z. Liang, X. Xu, Y. Yang, *Oxid. Med. Cell. Longev.* **2022**, 2886932 (2022). <https://doi.org/10.1155/2022/2886932>
- T. Joshi, A.K. Singh, P. Haratipour, A.N. Sah, A.K. Pandey, R. Naseri, V. Juyal, M.H. Farzaei, *J. Cell. Physiol.* **234**(10), 17212 (2019). <https://doi.org/10.1002/jcp.28528>
- C.N. Hsu, L.T. Huang, Y.L. Tain, *Int. J. Mol. Sci. J. Mol. Sci.* (2019). <https://doi.org/10.3390/ijms20225681>
- B.Y. Kim, H.S. Lim, Y.J. Kim, E. Sohn, Y.H. Kim, I. Koo, S.J. Jeong, *Sci. Rep.* **10**(1), 2658 (2020). <https://doi.org/10.1038/s41598-020-59537-8>
- X. Chen, J. Yang, M. Li, S. Zhu, M. Zhao, C. Yang, B. Liu, H. Gao, A. Lu, L. Ge, L. Mo, Z. Gu, H. Xu, *Redox Biol.* **54**, 102360 (2022). <https://doi.org/10.1016/j.redox.2022.102360>
- T. Hao, J. Li, F. Yao, D. Dong, Y. Wang, B. Yang, C. Wang, *ACS Nano* **11**(6), 5474 (2017). <https://doi.org/10.1021/acsnano.7b00221>
- C. Wang, M. Zhao, J. Xie, C. Ji, Z. Leng, Z. Gu, *Chem. Eng. J. Eng. J.* (2022). <https://doi.org/10.1016/j.cej.2021.131725>
- M. Ding, M. Li, E.M. Zhang, H.L. Yang, *Eur. Rev. Med. Pharmacol. Sci.* **24**(18), 9665 (2020). https://doi.org/10.26355/eur-rev_202009_23056
- W.S. Kuo, J.Y. Wang, C.Y. Chang, J.C. Liu, Y.T. Shao, Y.S. Lin, E.C. So, P.C. Wu, *Nanoscale Res. Lett.* **15**(1), 99 (2020). <https://doi.org/10.1186/s11671-020-03329-6>
- Y. Zhao, X. Shen, R. Ma, Y. Hou, Y. Qian, C. Fan, *Histol. Histopathol.* **36**(7), 725 (2021). <https://doi.org/10.14670/hh-18-316>
- V. Sergeeva, O. Kraevaya, E. Ershova, L. Kameneva, E. Malinovskaya, O. Dolgikh, M. Konkova, I. Voronov, A. Zhilenkov, N. Veiko, P. Troshin, S. Kutsev, S. Kostyuk, *Oxid. Med. Cell. Longev.* **2019**, 4398695 (2019). <https://doi.org/10.1155/2019/4398695>
- M. Zhao, C. Wang, J. Xie, C. Ji, Z. Gu, *Small* **17**(37), e2102035 (2021). <https://doi.org/10.1002/smll.202102035>
- W. Guo, X. Liu, L. Ye, J. Liu, K. Larwubah, G. Meng, W. Shen, X. Ying, J. Zhu, S. Yang, J. Guo, Y. Jia, M. Yu, *Materials* (2022). <https://doi.org/10.3390/ma15041349>
- E.S. Kovel, A.G. Kicheeva, N.G. Vnukova, G.N. Churilov, E.A. Stepin, N.S. Kudryasheva, *Int. J. Mol. Sci. J. Mol. Sci.* (2021). <https://doi.org/10.3390/ijms22126382>
- T. Zhang, R. He, X. Ding, M. Zhao, C. Wang, S. Zhu, Y. Liao, D. Wang, H. Wang, J. Guo, Y. Liu, Z. Zhou, Z. Gu, H. Hu, *Adv. Healthc. Mater.* (2023). <https://doi.org/10.1002/adhm.20230819>
- A. van der Pol, A. Gil, J. Tromp, H.H.W. Silljé, D.J. van Veldhuisen, A.A. Voors, E.S. Hoendermis, N. Grote Beverborg, E.M. Schouten, R.A. de Boer, R. Bischoff, P. van der Meer, *Cardiovasc. Res.* **114**(14), 1871 (2018). <https://doi.org/10.1093/cvr/cvy187>
- C. Cheng, H. Ma, G. Liu, S. Fan, Z. Guo, *Antioxidants* (2022). <https://doi.org/10.3390/antiox11050978>

23. T. Malina, E. Maršálková, K. Holá, R. Zbořil, B. Maršálek, J. Hazard. Mater. **399**, 123027 (2020). <https://doi.org/10.1016/j.jhazmat.2020.123027>
24. L. Zhu, J. Zang, B. Liu, G. Yu, L. Hao, L. Liu, J. Zhong, J. Cell. Physiol. **235**(10), 7392 (2020). <https://doi.org/10.1002/jcp.29641>
25. C. Chu, H. Zhang, S. Cui, B. Han, L. Zhou, N. Zhang, X. Su, Y. Niu, W. Chen, R. Chen, R. Zhang, Y. Zheng, J. Hazard. Mater. **369**, 180 (2019). <https://doi.org/10.1016/j.jhazmat.2019.02.026>
26. S.R. Mulay, Kidney Int. **96**(1), 58 (2019). <https://doi.org/10.1016/j.kint.2019.01.014>
27. D. Tang, R. Kang, T.V. Berghe, P. Vandenabeele, G. Kroemer, Cell Res. **29**(5), 347 (2019). <https://doi.org/10.1038/s41422-019-0164-5>
28. W. Zhang, C. Feng, H. Jiang, Ageing Res. Rev. **65**, 101207 (2021). <https://doi.org/10.1016/j.arr.2020.101207>
29. M. Li, W. Sun, R. Tian, J. Cao, Y. Tian, B. Gurrarn, J. Fan, X. Peng, Biomaterials **269**, 120532 (2021). <https://doi.org/10.1016/j.biomaterials.2020.120532>
30. L. Zhao, Z. Guo, P. Wang, M. Zheng, X. Yang, Y. Liu, Z. Ma, M. Chen, X. Yang, J. Cell. Mol. Med. **24**(1), 511 (2020). <https://doi.org/10.1111/jcmm.14758>
31. S. Gao, H. Li, H. Xie, S. Wu, Y. Yuan, L. Chu, S. Sun, H. Yang, L. Wu, Y. Bai, Q. Zhou, X. Wang, B. Zhan, H. Cui, X. Yang, Parasite Vector **13**(1), 260 (2020). <https://doi.org/10.1186/s13071-020-04104-3>
32. B. Mokhtari, R. Yavari, R. Badalzadeh, A. Mahmoodpoor, Can. J. Infect. Dis. Med. **2022**, 3277274 (2022). <https://doi.org/10.1155/2022/3277274>
33. X. Wang, Y. Ding, R. Li, R. Zhang, X. Ge, R. Gao, M. Wang, Y. Huang, F. Zhang, B. Zhao, W. Liao, J. Du, Nat. Commun. **14**(1), 1185 (2023). <https://doi.org/10.1038/s41467-023-36865-7>
34. A. Potruch, A. Schwartz, Y. Ilan, Adv. Gastroenter. **15**, 17562848221094214 (2022). <https://doi.org/10.1177/17562848221094214>
35. B. Du, L. Cao, K. Wang, J. Miu, L. Yao, Z. Xu, J. Song, Inflammation **43**(3), 1110 (2020). <https://doi.org/10.1007/s10753-020-01198-w>
36. E.A. Kang, H.I. Choi, S.W. Hong, S. Kang, H.Y. Jegal, E.W. Choi, B.S. Park, J.S. Kim, Biomedicines (2020). <https://doi.org/10.3390/biomedicines8110522>
37. M. Liu, J. Xie, Y. Sun, Cell. Mol. Neurobiol. **40**(6), 1029 (2020). <https://doi.org/10.1007/s10571-020-00791-9>
38. J. Zhang, Z.L. Luan, X.K. Huo, M. Zhang, C. Morisseau, C.P. Sun, B.D. Hammock, X.C. Ma, Int. J. Biol. Sci. **19**(1), 294 (2023). <https://doi.org/10.7150/ijbs.78097>
39. C.J. Luo, T. Li, H.L. Li, Y. Zhou, L. Li, Korean J. Physiol. Pha **27**(2), 143 (2023). <https://doi.org/10.4196/kjpp.2023.27.2.143>

Publisher's Note Springer Nature remains neutral with regard to jurisdictional claims in published maps and institutional affiliations.